16th Australasian Fluid Mechanics Conference
Crown Plaza, Gold Coast, Australia
2-7 December 2007

Numerical Study of the Behaviour of Wall Shear Stress in Pulsatile Stenotic Flows

A. Ooi[1], H. M. Blackburn[2], S. Zhu[1], E. Lui[1] and W. Tae[1]

[1]Department of Mechanical and Manufacturing Engineering
The University of Melbourne, Victoria, 3010 AUSTRALIA

[2]Department of Mechanical Engineering
Monash University, Victoria, 3800 AUSTRALIA

Abstract

This paper presents a numerical study of pulsatile flow through an axisymmetric stenosed artery. Numerical calculations of the incompressible Navier-Stokes equations were carried out in an axisymmetric geometry to investigate how the wall shear stress (WSS) is affected by varying levels of stenosis contractions and pulse periods (reduced velocity). It is found that the distribution and strength of the WSS is closely correlated with the position of the vortex ring formed at the stenosis. Each vortex ring generates high WSS at the stenosis walls and this high WSS propagate downstream with the vortex ring. As the vortex ring convects downstream, it loses its strength due to viscous effects and WSS decreases in magnitude. In general, the strength of the vortex ring increases with increasing stenosis levels which leads to higher WSS values on the walls. The effect of smaller pulse period is to reduce the distance between the vortex rings, thus increasing the spatial variation of WSS along the stenosed artery.

Introduction

Atherosclerotic disease, also known as atherosclerosis, is the most common form of cardiovascular diseases which occur mostly in larger arteries. Atherosclerosis is the hardening and narrowing of an artery due to lesions that cause plaque build-up on the wall that continues to accumulate over decades [16]. The plaque consists of fatty tissues, low-density lipoproteins (i.e. cholesterol), waste products and other substances and can appear to be spongy or relatively solid. It is the direct cause of strokes and heart-attacks and is the number one killer in developed countries.

This localized narrowing of the artery lumen is clinically known as a stenosis. Stenosis is primarily found in only a few specific locations in the human cardiovascular system, namely the carotid aorta sinus, the coronary arteries, the abdominal aorta, and the superficial femoral arteries [6]. At each of these sites, there exists region where the wall shear stress (WSS) rapidly oscillates in time. This correlation of stenosis occurring at regions of low and oscillatory WSS was first mentioned and observed by [4]. Since then, various investigators have carried out studies on how the WSS is affected in stenosed arteries ([2] , [8], [14], [1]). The importance of investigating oscillating WSS in abdominal aortic aneurysm has also been highlighted in the recent study conducted by [12]. In all these studies, it has been reported that the presence of a stenosis in the artery significantly alters the post-stenotic blood flow characteristics such as the flow velocity, pressure, WSS and derivatives (both spacial and temporal) of WSS. These flow variables change due to the development and break down of an unsteady shear layer which leads to the generation of vortex rings and the development of flow recirculation region downstream of the stenosis. The flow conditions downstream may further promote the growth of the stenosis or create a new site for the development of a new stenosis, and also the tendency for the plaque to rupture and block smaller arteries.

In addition to the presence of the stenosis, flow features in arteries are also influenced by the pulsatile nature of the cardiac cycle. This cyclic process of the heart creates pulsatile conditions in the arteries [6] which leads to many interesting flow features which is not present when the flow occurs in a continuous stream. A wide variety of pulsatile flow patterns are observed in various parts of the cardiovascular system. In order to obtain a better understanding of these flows, several investigators have performed high Reynolds number simulations of pulsatile stenotic flows. [9] and [8] studied the turbulent characteristics of a planar channel with a one-sided semicircular stenosis. [7] performed direct numerical simulation (DNS) of a pulsatile flow in a constricted round pipe and studied the evolution and instabilities of three dimensional vortical flow structures. More recently [2] carried out experimental and DNS study of pulsatile flow in a constricted channel and showed that the results are very sensitive to the inflow conditions upstream of the stenosis. [14] conducted numerical simulations of the three dimensional flow field and investigated how plaque rupture can be related to the geometry (morphology) of the stenosis vessel. These three-dimensional calculations are expensive as they are unsteady in nature and require many grid points to fully resolve all spatial and temporal scales in the calculations. A cheaper, but arguably less accurate, methodology of computing turbulent flow, would be to use the Reynolds Averaged Navier Stokes (RANS) approach where only the large length scales are simulated and the smaller length scales in the flow are modelled using a turbulence model. [15] and [11] used RANS methodology to study the effects of turbulence by using different RANS models and performing axisymmetric two-dimensional calculations of unsteady stenotic flows at high Reynolds numbers.

The main purpose of this paper is to investigate how the distribution and behaviour of the WSS can be related to the structures in the flow field. This is done by carrying out numerical simulations were carried out for a model of stenosis with different degree of stenosis and pulse period. Most of the calculations assumes that the flow field is axisymmetric but results from fully three-dimensional calculations are also presented. Details of the calculations are described in the next section.

Numerical Model

In this study, the fluid is assumed to be Newtonian and incompressible. Thus, flow physics is simulated by solving the incompressible Navier-Stokes equations. A spectral element method is utilised which allows for very accurate simulation of flows in a relatively complex geometry. See [3] for more details on the numerical algorithm.

The geometry of the stenosis artery is idealized as a smooth constriction on a long rigid straight axisymmetric pipe. The important parameters for this problem are the pipe diameter, D and the diameter of the throat, $D_{\min}$ (see Fig. 1), which determines

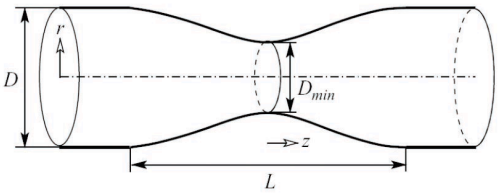

Figure 1: Geometrical parameters of the simulations

the degree of stenosis,

$$S = \frac{D - D_{\min}}{D}. \tag{1}$$

The computational meshes used in the numerical calculations are adopted from [13]. Computational cells are smaller close to the walls in order to resolve the sharp velocity gradients at the walls. For the case with $S = 25\%$ and $S = 50\%$, mesh consists of of 743 elements and the length of the computational domain is $50D$. For all meshes used, the throat of the stenosis is located at $z/D = 5$. The mesh for $S = 75\%$ is similar but the axial domain is longer, up to $75D$ and consists of 915 elements. A longer axial domain is needed to ensure that the stronger vortex rings which form at the stenosis have diffused sufficiently before they exit the computational domain. For each spectral element, the order of the polynomial $N_p = 10$ is used. This corresponds to approximately 74300 local degrees of freedom (for the semi plane) for the $S = 25\%$ and $S = 50\%$ mesh and corresponds to approximately 91500 local degrees of freedom for the $S = 75\%$ mesh.

The axisymmetric inflow axial velocity, $u(r,t)$, with temporal period T used in the simulations has a sectional average of

$$\overline{u}(t) = \frac{8}{D^2}\int_0^{D/2} u(r,t) r dr \tag{2}$$

and temporal average given by

$$\overline{u}_m = \frac{1}{T}\int_0^T \overline{u}(t) dt. \tag{3}$$

In this paper two independent dimensionless groups can be defined to characterize the inflow, the reduced velocity, U_{red} and the Reynolds number Re are defined by

$$\begin{aligned} U_{\text{red}} &= \frac{\overline{u}_m T}{D} \\ Re &= \frac{\overline{u}_m D}{\nu}. \end{aligned} \tag{4}$$

ν is the kinematic viscosity of the fluid which is assumed to be constant in this study. U_{red} can be interpreted as the convective length that the mean flow travels in one pulse period T and therefore introduces an axial length scale into the parameter. It can also be treated as a dimensionless pulse period [13].

Flow at three different stenosis levels (S =25%, 50%, and 75%), and four pulsatile inflows with different reduced velocities (U_{red} =0.875, 2.5, 3.25, and 10) will be investigated. The values of U_{red} used in this study is quite close to physiological conditions. Under normal resting conditions, [10] has suggested that $U_{\text{red}} \approx 3.25$. All simulations will be carried out at $Re = 400$ which is slightly lower than what has been previously measured in vivo (the expected values of physiological Reynolds numbers in the abdominal aorta are expected to range from 550 to 1150 ([10])).

For most of the results shown in this paper, the flow field is assumed to be axisymmetric. In reality, flows at $Re = 400$ can be expected to be fully three-dimensional. Towards the end of this paper, results from preliminary three-dimensional are presented and compared with data from the axisymmetric calculations.

Results and discussion

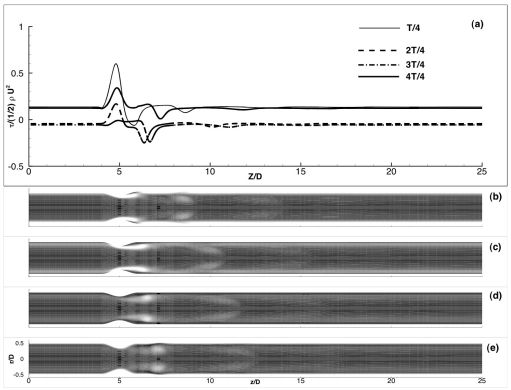

Figure 2: Vorticity contours for the pulsatile flow through the $S = 25\%$ model with $U_{\text{red}} = 2.5$. (a) Normalised instantaneous WSS distribution (b) $t = nT/4$, (c) $t = n2T/4$,(d) $t = n3T/4$ and (e) $t = n4T/4$. Contour levels are from -1 to 20 with black indicating low and high contour levels are indicated by white.

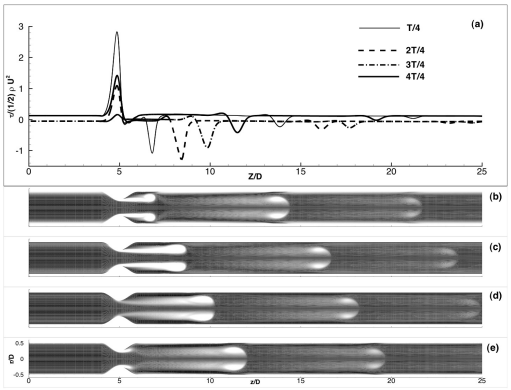

Figure 3: Vorticity contours for the pulsatile flow through the $S = 50\%$ model with $U_{\text{red}} = 2.5$. (a) Normalised instantaneous WSS distribution (b) $t = nT/4$, (c) $t = n2T/4$,(d) $t = n3T/4$ and (e) $t = n4T/4$. Contour levels are from -1 to 30 with black indicating low and high contour levels are indicated by white.

Contours of azimuthal vorticity and the instantaneous spatial distribution of the WSS for S=25%, 50% and 75% are shown in Figs. 2, 3 and 4 respectively. Data shown in these figures are computed with $U_{\text{red}} = 2.5$. Only one period is shown because the flow is periodic with period, T. Note that important features of the flow field occur further downstream for the $S = 75\%$ cases as compared to cases with $S = 25\%$ and 50%. Hence, in order to illustrate all features of the flow field 4 show a longer domain (up till ($z = 50D$)).

From $0 < t < T/4$, a jet is form in the proximal of the post-stenotic region. There is a roll-up of the circular vortex sheet

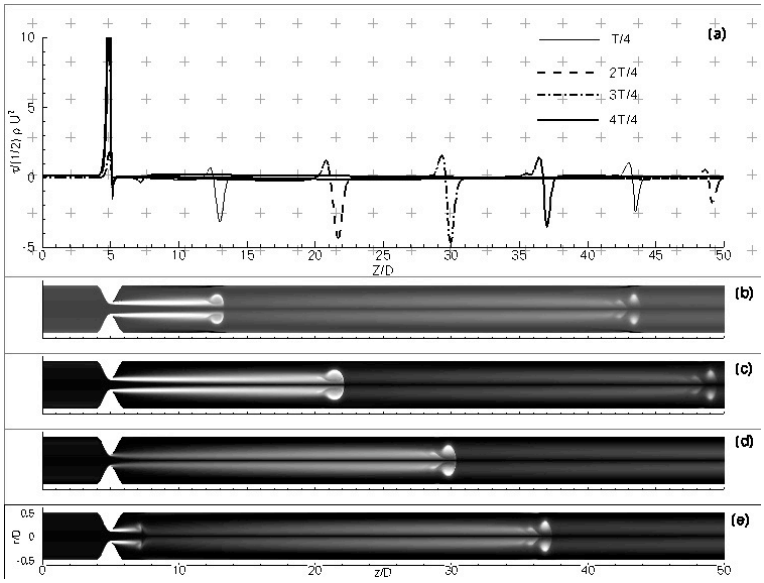

Figure 4: Vorticity contours for the pulsatile flow through the $S = 75\%$ model with $U_{\text{red}} = 2.5$.(a) Normalised instantaneous WSS distribution (b) $t = nT/4$, (c) $t = n2T/4$,(d) $t = n3T/4$ and (e) $t = n4T/4$. Contour levels are from -50 to 200 with black indicating low and high contour levels are indicated by white.

to form a vortex ring. The strength of the vortex ring is greatly dependent on S. For larger values of S, there is faster flow velocities (due to the smaller area) at the throat which leads to the formation of stronger vortex rings. When there is flow deceleration at the inflow ($T/4 < t < 3T/4$) there is a continuation of the build up of the circular vortex ring which causes it to further interact with the wall. At $t = 3T/4$, the vortex ring seems to be still connected to the lip of the constriction through the presence of the round shear layer. As can be seen by comparing the data in Figs. 2, 3 and 4, the length of this circular shear layer is seem to increase with S. During $3T/4 < t < 4T/4$, the shear layer detaches from the throat and the vortex ring propagate downstream. As the vortex ring is convected downstream, its strength decreases due to viscous effects. The radius of the vortex ring also appear to shrink as it propagates downstream. This sequence of flow events is repeated for each pulse cycle. It is also clear that the vorticity distribution upstream from stenosis is not influenced by S.

Figures 2, 3 and 4 also shows the instantaneous spatial distribution of the WSS. For all cases, the WSS distribution upstream of the stenosis do not change with S. For all S, upstream of the stenosis, the WSS is positive at $t = T/4$ and $4T/4$ and negative at $t = 2T/4$ and $3T/4$. This indicate that upstream boundary condition has reverse flow very close to the wall between $t = 2T/4$ and $3T/4$. Downstream of the throat, it can be seen that the WSS is nearly constant along the tube at any time. The only exception where there are large variation of WSS is near the throat and in the vicinity of the vortex rings. Maximum magnitude of the WSS occur at the throat due to the high flow velocity. Hence the magnitude of the WSS at the throat varies with S with larger values of S giving rise to larger velocities and larger WSS at the throat. Downstream of the stenosis, the formation and interaction of the vortex ring with the wall causes the large local variation in the WSS. Figures 2 to 4 show that the the local minima of the WSS correlate very well with the location of the vortex rings. As the vortex rings convect downstream, the WSS tend to increase in magnitude and then decrease in magnitude. The magnitude of the WSS downstream of the stenosis in the vicinity of the vortex ring is approximately 2-3 times smaller in magnitude than the value of the WSS at the throat.

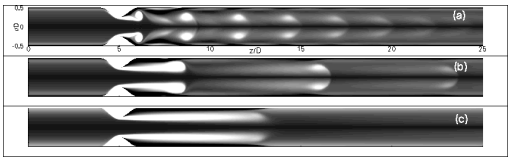

Figure 5: Vorticity contours for the pulsatile flow through the $S = 50\%$ model with $U_{\text{red}} = 0.875$ (a), $U_{\text{red}} = 2.5$ (b), $U_{\text{red}} = 10$ (c). Contour levels are from -50 to 200 with black indicating low and high contour levels are indicated by white. Taken at time $t = nT/2$.

The effect of changing U_{red} is illustrated in Fig. 5 which shows contours of azimuthal vorticity for three U_{red} (0.875, 2.5 and 10) at $= n2T/4$ for simulations carried out at $Re = 400$ and $S = 50\%$. It is clear that the distance between successive vortex rings is dependent on U_{red}. Low U_{red} values mean shorter pulse period is shorter, thus the distance between successive vortex rings is shorter. Since it has been shown earlier that the WSS downstream of the throat is closely correlated to the location of the vortex rings, it is also clear that there larger variation in the WSS profile for lower U_{red} values.

Figure 6 show how the time averaged WSS vary with different degree of stenosis for $U_{\text{red}} = 2.5$. The averaging was calculated for one complete period of flow pulsation at the inflow. Figure 6(b) is the zoomed in version of Figure 6(a) . The data shows large positive mean WSS values at the throat (located at $z/D = 5$), with magnitude increasing with S. Downstream of the throat, there are regions where the WSS is negative which indicates the occurrence of mean recirculation region. In Fig. 6(b), it is clear that for S =25%, there is only a small mean recirculation region while the data for $S = 75\%$ shows that there is a large mean recirculation region, at approximately $60D$.

Comparison with Data from Three Dimensional Simulations

Thus far, all data presented are computed from axisymmetric

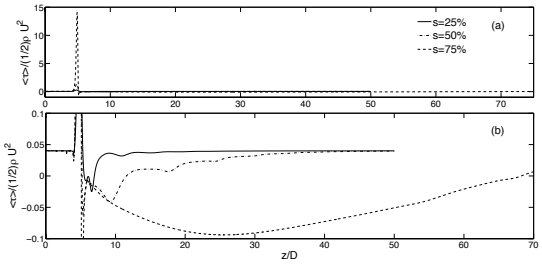

Figure 6: Mean value of spatial wall shear stress variation of pulsatile flow with $U_{\text{red}} = 2.5$ for different degree of stenosis (a). (b) is a zoomed in view of (a).

(two-dimensional) simulations. In reality, all flows are three-dimensional due mainly to the growth of instability modes in the flow field. Thus, it would be instructive to compare results from the axisymmetric simulations with data from three dimensional simulations in order to study the effects of these instability modes on the flow structure and the distribution of WSS. Figure 7 compares the 2d and 3d vorticity distribution. As can be seen, the vorticity distribution is similar up till $z \approx 7D$. In the three dimensional simulations, the vortex ring break down. This phenomena will no doubt influence the WSS distribution which is shown in Fig. 8. It is clear that the vortex break down produces a more homogeneous distribution of WSS downstream of the throat. Figure 8 illustrates the three dimensional vortex structures identified using the λ_2 definition suggested by [5] with the corresponding tangential WSS distribution. Comparing Fig. 8(b) with Fig. 3(a) shows that similar to the axisymmetric simulations, the maximum WSS occur at the throat. Downstream of the throat, the WSS distribution is very "patchy" owing to the break down of the vortex ring in the three-dimensional simulations. This is more clearly illustrated in Fig. 9 which shows comparison between the azimuthally averaged WSS of the full three-dimensional simulation with the WSS computed from the corresponding two-dimensional simulation. It is clear that the distribution of the WSS is very similar upstream of the throat. The WSS directly downstream of the throat is the same, up till region where there is a breakdown of the vortex ring. It is also clear that in the three-dimensional simulations, there is no local minima of the WSS downstream of the stenosis.

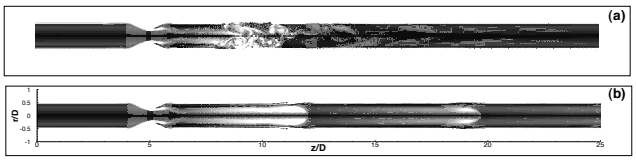

Figure 7: (a) contours of vorticity squared from 3d simulations. (b) contours of azimuthal vorticity from 2d simulations

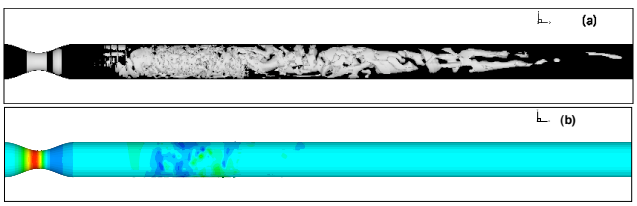

Figure 8: Isosurfaces of λ_2 for S =50% and $U_{\text{red}} = 2.5$(a). Corresponding normalized tangential wall shear stress $(\tau/((1/2)\rho U^2))$ distribution (b). Contour levels are from -0.2 (blue) to 1.4 (red).

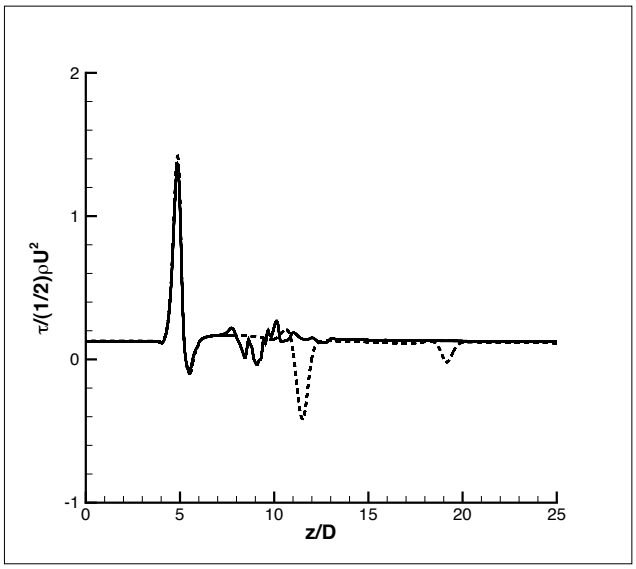

Figure 9: ——— Azimuthally averaged wall shear stress of the instantaneous three-dimensional field. – – – – WSS computed from the two-dimensional simualations

Conclusions

The objective of this current study is to provide overall flow characteristics and wall shear stress distribution of pulsatile flow through a stenosed tube. Simulations were carried out in an axisymmetric domain with varying degree of stenosis, S, and reduced velocities, U_{red}. Larger values of S, lead to higher wall shear stress values and the location of large WSS values correlate with the location of the vortex rings. The distance between the vortex rings depend greatly on U_{red} and S. The vortex rings are closer together for smaller values of U_{red} and S values. This will lead to larger variation in WSS distribution on the wall.

Preliminary data from three dimensional simulation shows that data from two dimensional calculations is only valid up till a region directly downstream of the stenosis. Data from three dimensional calculations show that far downstream of the stenosis, the vortex ring break down to produce small scale vortex structures. This would likely lead to a more homogeneous distribution of WSS when compared to data from two dimensional simulations which shows a very localised distribution of large WSS values.

Acknowledgements

The authors would like to thank the Victorian Partnership for Advanced Computing (VPAC) and the Australian Partnership for Advanced Computing (APAC) for providing the computer time to carry out this work.

References

[1] Ahmed, S. A. and Giddens, D. P., Velocity measurements in steady flow through axisymmetric stenoses at moderate reynolds numbers, *J. Biomechanics*, **16**, 1983, 505–516.

[2] Beratlis, N., Balaras, E., Parvinian, B. and Kiger, K., A numerical and experimental investigation of transitional pulsatile flow in a stenosed channel, *J. Biomechanical Engineering*, 1147–1157.

[3] Blackburn, H. M. and Sherwin, S. J., Formulation of a galerkin spectral element-fourier method for three-

dimensional incompressible flows in cylindrical geometries, *J. Computational Physics*, **197**, 2004, 759–778.

[4] Caro, C. G., Fitz-gerald, J. M. and Schroter, R. C., Atheroma and arterial wall shear: observation, correlation and proposal of a shear dependant mass transfer mechanism for atherogenesis., *Proc. R. Soc. Land. B*, 109–159.

[5] Jeong, J. and Hussain, F., On the identification of a vortex, *J. Fluid Mech.*, **285**, 1995, 69–94.

[6] Ku, D. N., Blood flow in arteries, *Annu. Rev. Fluid Mech.*, **29**, 1997, 399–434.

[7] Mallinger, F. and Drikakis, D., Instability in three-dimensional, unsteady, stenotic flows, *Int. J. Heat and Fluid Flow*, **23**, 2002, 657–663.

[8] Mittal, R., Simmons, S. P. and Najjar, F., Numerical study of pulsatile flow in a constricted channel, *J. Fluid Mech.*, **485**, 2003, 337–378.

[9] Mittal, R., Simmons, S. P. and Udaykumar, H. S., Application of large-eddy simulation to the study of pulsatile flow in a modeled arterial stenosis, *J. Biomechanical Engineering*, **123**, 2001, 325–332.

[10] Moore, J. E., Maier, S. E., Ku, D. K. and Boesiger, P., Hemodynamics in the abdominal aorta: a comparison of in vitro and in vivo measurements, *J. Appl. Physiol.*, **76**, 1994, 1520–1527.

[11] Ryval, J., Straatman, A. G. and Steinman, D. A., Two-equation turbulence modeling of pulsatile flow in a stenosed tube, *J. Biomechanical Engineering*, **126**, 2004, 625–635.

[12] Salsac, A. V., Sparks, S. R., Chomaz, J. M. and Lasheras, J. C., Evolution of the wall shear stresses during the progressive enlargement of symmetric abdominal aortic aneurysms, *J. Fluid Mech.*, **560**, 2006, 19–51.

[13] Sherwin, S. J. and Blackburn, H. M., Three-dimensional instabilities and transition of steady and pulsatile flows in an axisymmetric stenotic tube, *J. Fluid Mech.*, **533**, 2005, 297–327.

[14] Stroud, J. S., Berger, S. A. and Saloner, D., Influence of stenosis morphology on flow through severely stenotic vessels: implications for plaque rupture, *J. Biomechanics*, **33**, 2000, 443–455.

[15] Varghese, S. S. and Frankel, S. H., Numerical modeling of pulsatile turbulent flow in stenotic vessels, *J. Biomechanical Engineering*, **125**, 2003, 445–460.

[16] Wootton, D. M. and Ku, D. N., Fluid mechanics of vascular systems, diseases and thrombosis, *Annu. Rev. Biomed. Eng.*, **1**, 1999, 299–329.